HHS Public Access

Author manuscript

Biomech Model Mechanobiol. Author manuscript; available in PMC 2019 February 01.

Published in final edited form as:

Biomech Model Mechanobiol. 2018 February ; 17(1): 181–189. doi:10.1007/s10237-017-0953-z.

EFFECT OF AGING ON MECHANICAL STRESSES, DEFORMATIONS, AND HEMODYNAMICS IN HUMAN FEMOROPOPLITEAL ARTERY DUE TO LIMB FLEXION

Anastasia Desyatova[a], **Jason MacTaggart**[a], **Rodrigo Romarowski**[b], **William Poulson**[a], **Michele Conti**[b], and **Alexey Kamenskiy**[a,*]

[a]Department of Surgery, University of Nebraska Medical Center, Omaha, NE

[b]Department of Civil Engineering and Architecture, University of Pavia, Italy

Abstract

Femoropopliteal artery (FPA) reconstructions are notorious for poor clinical outcomes. Mechanical and flow conditions that occur in the FPA with limb flexion are thought to play a significant role, but are poorly characterized. FPA deformations due to acute limb flexion were quantified using a human cadaver model, and used to build a finite element model that simulated surrounding tissue forces associated with limb flexion-induced deformations. Strains and intramural principal mechanical stresses were determined for seven age groups. Computational fluid dynamics analysis was performed to assess hemodynamic variables. FPA shape, stresses, and hemodynamics significantly changed with age. Younger arteries assumed straighter positions in the flexed limb with less pronounced bends and more uniform stress distribution along the length of the artery. Even in the flexed limb posture, FPAs younger than 50 years of age experienced tension, while older FPAs experienced compression. Aging resulted in localization of principal mechanical stresses to the Adductor Hiatus and popliteal artery below the knee that are typically prone to developing vascular pathology. Maximum principal stresses in these areas increased 3–5 fold with age with largest increase observed at the Adductor Hiatus. Atheroprotective wall shear stress reduced after 35 years of age, and atheroprone and oscillatory shear stresses increased after the age of 50. These data can help better understand FPA pathophysiology and can inform the design of targeted materials and devices for Peripheral Arterial Disease treatments.

Keywords

femoropopliteal artery; limb flexion; stress; deformation; hemodynamics; aging

[*]Corresponding author Correspondence and Reprints requests to: Alexey Kamenskiy, Department of Surgery, 987690 Nebraska Medical Center, Omaha, NE 68198-7690, Tel: +1 (402) 559-5100, Fax: +1 (402) 559-8985, Alexey.Kamenskiy@unmc.edu.

DISCLOSURES

Funding: Research reported in this publication was supported in part by National Heart, Lung, And Blood Institute of the National Institutes of Health [grant numbers R01 HL125736 and F32 HL124905].

Conflict of interest: The authors declare that they have no conflict of interest in relation to this submission.

1. INTRODUCTION

The femoropopliteal artery (FPA) is the largest artery in the limb supplying blood to the tissues of the lower extremity. It includes the more proximal superficial femoral artery (SFA) and the more distal popliteal artery (PA) separated by the Adductor Hiatus (AH), a tendinous channel between the adductor magnus muscle and the femur. The AH and the PA are the most common sites for atherosclerotic obstruction that reduces blood flow to the lower limbs(Watt 1965) - a condition known as peripheral arterial disease (PAD). PAD is one of the major contributors to public health burden and is one of the most expensive vascular diseases to treat (Mahoney et al. 2008). The high cost is mostly attributed to large numbers of peripheral vascular operations and interventions that fail and require reintervention (Adam et al. 2005; Schillinger et al. 2006; Conte et al. 2006; Schillinger et al. 2007).

High failure rates of FPA interventions compared to other arterial beds suggest that local factors unique to the FPA may have a significant role. The two major differences between the leg artery and other arteries in the body, are the complex biomechanical environment that imposes bending, twisting, and compression deformations on the FPA with limb flexion and extension (Ansari et al. 2013; MacTaggart et al. 2014; Desyatova et al. 2017b; Poulson et al. 2017), and slow complex flow in the flexed limb posture (Newcomer et al. 2008). Severe FPA deformations with limb flexion may contribute to arterial wall injury(Clowes et al. 1983; MacTaggart et al. 2014), mechanical failure of the repair device due to fatigue and fracture(Iida et al. 2006; Higashiura et al. 2009; Ansari et al. 2013), and atherogenic flow patterns with low and oscillatory shear(Malek et al. 1999). In addition, these mechanical and flow characteristics may change with age as FPA loses longitudinal pre-stretch and becomes more tortuous in the flexed limb posture(Kamenskiy et al. 2016). This can contribute to higher intramural stresses, and lower flow shear stress that can switch the phenotype from atheroprotective (>1.5 Pa) to atheroprone (<0.4 Pa)(Malek et al. 1999). All these factors acting synergistically may lead to deleterious cellular and biochemical responses, culminating in restenosis and reconstruction failure(Dunlop and Santos 1957; Palma 1959; Watt 1965; Clowes et al. 1983; Wensing et al. 1998).

While deformations of the FPA have recently been characterized(MacTaggart et al. 2014; Desyatova et al. 2017b; Poulson et al. 2017), mechanical stresses and flow hemodynamics associated with these deformations have not yet been determined. Our recent study(Desyatova et al. 2017a) focused on developing a computational framework to study limb flexion-induced FPA stresses and strains, and the goal of the current work was to apply this approach to determine how limb flexion-induced arterial stresses, deformations, and hemodynamics change with age.

2. METHODS

2.1 FPA deformations with limb flexion, mechanical properties, and constitutive formulation

Arterial deformations were measured using an 89-year-old male human cadaver model, custom-designed intra-arterial markers, and Computed Tomography (CT) imaging. Details of the model and the method are provided elsewhere(MacTaggart et al. 2014; Desyatova et

al. 2017b; Poulson et al. 2017). Briefly, limbs were imaged in the standing (180° at the knee, straight) and gardening (60° at the knee, acutely bent) postures using clinical CT (Figure 1), and image segmentation was used to determine spatial marker positions. These positions were used to measure FPA deformations with limb flexion.

A large set of 579 fresh FPA specimens from 351 donors 13–82 years old was used to determine the mechanical properties and *in situ* pre-stretch of FPAs from seven age groups. Details of these biaxial tests are provided in Kamenskiy et al (Kamenskiy et al. 2017). Four-fiber-family invariant-based material model was used to describe the FPA behavior(Desyatova et al. 2017a; Kamenskiy et al. 2017). Strain energy density U for this material has the form:

$$U=\frac{C_0}{2}(\bar{I}_1-3)+\frac{1}{D_1}\left(\frac{J^2-1}{2}-\ln J\right) + \frac{c_1^{el}}{4c_2^{el}}\left\{\exp\left[c_2^{el}\left(I_4^{el}-1\right)^2\right]-1\right\} + \frac{c_1^{smc}}{4c_2^{smc}}\{\exp[c_2^{smc}(I_4^{smc}-1)^2]-1\}+\frac{c_1^{col}}{4c_2^{col}}\sum_{i=3,4}\left\{\exp\left[c_2^{col}\left(I_4^{i}-1\right)^2\right]-1\right\} \quad (1)$$

Here, C_0 is the initial shear modulus of the isotropic ground substance, $c_1^i>0$ is a stress-like material parameter for i^{th} fiber family, c_2^i is a dimensionless material parameter for i^{th} fiber family, and I_4^i is a fourth invariant, equal to the square of the stretch in the i^{th} fiber direction $I_4^i=\mathbf{M}^i\left(\boldsymbol{C}\mathbf{M}^i\right)^2=\lambda_i\left(\mathbf{M}^i\right)^2$. $\mathbf{M}^i$ is a unit vector of the i^{th} fiber direction in the reference configuration making an angle γ^i with the longitudinal direction. $\boldsymbol{C}$ denotes the right Cauchy-Green tensor. Modified anisotropic formulation with full anisotropic invariants(Nolan et al. 2014) was adopted to properly model material response under volumetric deformations.

Fiber families representing histological FPA structure(Kamenskiy et al. 2016) include elastin oriented along the longitudinal direction (γ^{el} = 0); smooth muscle cells oriented in the circumferential direction (γ^{smc} = π/2); and two families of collagen fibers oriented helically at angle ±γ. Constitutive model parameters (c_0, $c_1^{el}, c_2^{el}, c_1^{smc}, c_2^{smc}, c_1^{col}, c_2^{col}$, γ) for different age groups along with the age-specific *in situ* longitudinal pre-stretch are provided in Kamenskiy et al(Kamenskiy et al. 2017). Parameter D_1 was chosen such that the ratio of initial bulk modulus to initial shear modulus was K_0/C_0 = 20 to satisfy recommendations for explicit analysis.

2.2 Finite Element Model of the FPA deformations with limb flexion

Finite element (FE) analysis using Abaqus 6.14/Explicit (Simulia, Dassault Systemes, Waltham, MA) was employed to quantify intramural principal mechanical stresses due to limb-flexion induced FPA deformations. Details of the model are provided elsewhere(Desyatova et al. 2017a), but methodology will be briefly summarized below. FPA was modeled as a tube lofted along the arterial centerline in the straight limb posture. The

shape of the artery in the straight position was assumed the same across all age groups, but was uniformly scaled down using an inverse of age-specific *in situ* pre-stretch $\lambda_z^{in\ situ}$ to simulate axial retraction upon excision to a stress-free configuration. Longitudinal pre-stretch varied from 1.53 for the youngest to 1.10 for the oldest group (Kamenskiy et al. 2017).

Since arterial diameters and wall thickness change with age(Kamenskiy et al. 2017), pressurization experiments were performed on 32 human FPAs 15–72 years old (average age 50±18 years old) to determine correct arterial dimensions for the model. Arteries were pressurized with formalin at 120 mmHg for 24 hours, and pressure-fixed cross-sections were used to measure internal diameters and wall thickness. Diameters ranged from 4.7mm in the youngest age group, to 6.7mm in the oldest following a linear relation $D = 0.034 \cdot + 4.106$ (mm), while wall thickness remained approximately 1mm for FPAs younger than 50 years old, and then increased at a rate of 0.1 mm per decade of life. Along with diameters and wall thickness, material properties in the model were also adjusted for each age group based on data provided in Kamenskiy et al (Kamenskiy et al. 2017). In order to determine whether pre-stretch reduction or material stiffening have stronger effect on the deformed shape, a constant pre-stretch of 1.10 was used in combination with varying material properties.

Deformation field associated with limb flexion was defined by the differences between the FPA centerlines in the straight and flexed limb postures. However, the deformed shape may be different in younger arteries because they are more compliant and have higher longitudinal pre-stretch. To account for this, a set of springs and dashpots was utilized instead of directly applying the displacement field. Artery was sectioned along the centerline in locations corresponding to the intra-arterial markers and midway between the markers. These sections were constrained to move as rigid bodies with their reference points serving as attachment points of springs and dashpots. Displacement boundary conditions were prescribed to the opposite end of springs and dashpots. Spring stiffness was set to 50 kN/m and dashpot coefficient to 0.05 kNs/m as determined previously(Desyatova et al. 2017a).

Deformation of the FPA from the straight into the flexed configuration was performed quasi-statically by applying displacements to spring reference points using smooth step amplitude. Soft springs allowed the artery to assume different shapes depending on the stiffness and *in situ* longitudinal pre-stretch of the FPA in each age group. Kinetic and internal energies were monitored to ensure that kinetic energy stayed within 5% of the internal energy during the entire loading process. Four-node linear reduced integration shell elements (S4R) were used to create an FE mesh. Enhanced hourglass control was used to avoid mesh instability, and convergence study was performed to determine optimum mesh size. Four-fiber FPA constitutive model was implemented using material user subroutine VUMAT for shell elements and validated using experimental data. Out-of-plane shear stiffness was set at $k_{11} = k_{22} = 1\ MPa$ $k_{12} = 0$ for all simulations(Desyatova et al. 2017a). Local material orientation was defined along the longitudinal (axis 1), circumferential (axis 2), and transverse (axis 3) directions.

Effects of age on the stress-strain state were assessed by comparing maximum principal stresses and centerline deformations across all seven age groups. Maximum principal

stresses were calculated through the wall thickness in each element of the model except those near the rigid rings where stress values were influenced by edge effects. Maximum and median values of maximum principal stress along the arterial segment were reported. Axial deformation of the artery was calculated for each pair of intra-arterial markers (Figure 1), and for the entire SFA and PA segments. Calculation was done relative to the pre-stretched *in situ* length in the straight limb posture. Since *in situ* configuration is not stress-free due to presence of longitudinal pre-stretch, an additional axial deformation measurement relative to the *excised* stress-free length was obtained. Finally, arterial bending was assessed by calculating centerline curvature and tortuosity. Tortuosity was defined as the ratio of centerline length to the shortest distance between the centerline endpoints, and curvature was measured as a reciprocal of the centerline-inscribed radii.

2.3 Computational Fluid Dynamics in the FPA with limb flexion

Computational Fluid Dynamics (CFD) analysis was performed to assess the effects of limb flexion on the FPA hemodynamics. Arterial centerlines in the flexed limb posture obtained from FEA were extracted for all seven age groups, and surface lofting along the centerline was performed with age-specific diameters used in the FEA model. Volume mesh was created with open source VMTK software suite(Antiga et al. 2008), and the Navier-Stokes equations were solved with C++ FE library lifeV(Passerini et al. 2013). Blood was modeled as a Newtonian fluid with 1060 kg/m^3 density and 0.0035 $Pa{\cdot}s$ viscosity. The inflow boundary condition represented a typical femoral artery pulsatile waveform(Patel et al. 1965) that was assumed the same for all age groups. Stress-free condition was imposed at the distal end of the FPA. Time averaged wall shear stress (TAWSS) and oscillatory shear index (OSI) were calculated to assess FPA hemodynamics. Time convergence was achieved by simulating six cycles with a time step of 0.000642 sec. Solutions were mesh independent with <5% difference in TAWSS and <10% in OSI. The number of elements depended on the age group and varied from $720{\cdot}10^3$ to $1555{\cdot}10^3$.

3. RESULTS

Figure 1 demonstrates shapes of the FPA in the standing and gardening postures obtained with CT imaging. Limb flexion produced severe FPA deformations primarily at the AH and in the PA below the knee. FE modeling demonstrated that tortuosity of the FPAs in the flexed limb posture increased with age, particularly in the areas around the AH and in the PA below the knee (Figure 2). However, reduced tortuosity in younger FPAs was primarily determined by pre-stretch rather than more compliant material properties. In fact, when a pre-stretch of 1.10 that is characteristic of a 71–80 year old FPA was used with material characteristics from an 11–20 year old artery, FPA tortuosity in the flexed limb posture was even larger than in the oldest age group.

Distribution of the *in situ* and *excised* axial deformations (%) along the normalized length of the artery for seven age groups is demonstrated in Figure 3A–B. Change in axial deformation with age for both the SFA and the PA segments is summarized in Figure 3C–D, with solid lines representing average and dashed lines representing peak values. *In situ* axial compression decreased with age while *excised* compression increased. Relative to the stress-

free *excised* configuration (Figure 3B,D), arteries younger than 50 years of age experienced mostly tension (up to 25%) in the flexed limb posture with only the AH and several areas in the PA below the knee experiencing compression of 3–12% depending on age group. On the contrary, older arteries were in compression along most of their length reaching as high as 22% compression at the AH and in the PA. With respect to the pre-stretched *in situ* configuration, FPAs in the flexed limb posture always experienced axial compression with peak values ranging from 35% to 29% depending on the age group (Figure 3A,C).

Change in tortuosity of the FPA with age is shown in Figure 4A. Distribution of the FPA curvature along the normalized length of the artery for three age groups is presented in Figure 4B. There is a gradual increase in tortuosity with age from 1.39 in the youngest group to 1.55 in the oldest group. Increased tortuosity reflected changes in the FPA shape demonstrating more pronounced peaks in the curvature graph for older arteries (Figure 4B).

Distribution of maximum principal stresses in the artery is demonstrated in Figure 2 panel A for three age groups. Stresses in the vicinity of rigid rings have artificially high values due to edge effects; therefore, they were excluded from the analysis. Figure 2 demonstrates that areas of stress concentration change with age. In younger FPAs stresses are higher in the relatively straight segments of the artery that experience stretch (i.e. proximal PA), whereas in the older FPAs high stresses are localized to the areas of acute bends, i.e. at the AH and in the PA below the knee. Dependence of maximum stresses on age is demonstrated in Figure 5A. Maximum stresses do not change significantly around the AH in arteries younger than 40 years of age and average 54 kPa. Older arteries experience a sharp increase in stress up to 240 kPa in the oldest group. Unlike stresses in the distal SFA, stresses below the knee are increasing with age even in younger arteries, but level at approximately 200 kPa starting at the age of 50 years old. Contrary to the maximum stresses, median intramural stresses decrease with age for both the SFA and the PA primarily due to nonuniform stress distribution in older FPAs and large areas of artery that experience no or very little stress (Figure 5B and Figure 2). For the youngest age group median stresses average 21 kPa and 21 kPa in the SFA and PA respectively. They gradually decrease with age to become less than 5 kPa.

Analysis of hemodynamics is presented in Figure 2 panel B, while changes in TAWSS and OSI are presented in Figure 6 as a percentage of the total surface area. Atheroprotective (>1.5 Pa) and atheroprone (<0.4 Pa) TAWSS were defined according to Malek et al(Malek et al. 1999), and the results demonstrate a significant reduction of atheroprotective TAWSS by 35 years of age and exponential increase in atheroprone TAWSS after 50 years of age. In addition, OSI monotonically increases during the entire lifespan, but the increase is accelerated after 50 years of age. In middle-aged arteries low TAWSS and high OSI are localized primarily to the AH and PA below the knee. In older age groups the majority of the artery is experiencing atheroprone TAWSS with no atheroprotective TAWSS and significantly more oscillatory flow.

4. DISCUSSION

Aging is one of the primary non-modifiable risk factors for vascular disease (Learoyd and Taylor 1966; Jani and Rajkumar 2006; Greenwald 2007; O'Rourke 2007; Lakatta et al. 2009; Lee and Oh 2010; Kamenskiy et al. 2017). In human FPA it is associated with accumulation of collagen and degradation and fragmentation of elastin that results in reduction of longitudinal pre-stretch(Kamenskiy et al. 2015; Kamenskiy et al. 2016; Kamenskiy et al. 2017). This in turn may lead to more pronounced arterial kinking during limb flexion, high stress concentrations, abnormal flow, and deleterious cellular and biochemical responses potentially culminating in vascular disease or reconstruction failure(Dunlop and Santos 1957; Palma 1959; Watt 1965; Clowes et al. 1983; Wensing et al. 1998; MacTaggart et al. 2014). In this study we have investigated the effect of aging on limb flexion-induced FPA deformations, stresses, and hemodynamics using computational modeling.

Our results demonstrate that the shape of the artery, its intramural stresses, and blood flow hemodynamics significantly change with age. Younger arteries assume straighter positions in the flexed limb with less pronounced bends in the distal SFA near the AH, and in the PA below the knee. This effect was also observed experimentally by Cheng et al(Cheng et al. 2010) who found less FPA bending in younger patients with limb flexion. Our results demonstrate that on average young FPAs experience 24% axial compression *in situ* with maximum values reaching 34%. Old FPAs on average experience only 15% compression with maximum values reaching 29%. Decrease in *in situ* compression with age is mainly associated with significant reduction of longitudinal pre-stretch, from 1.53 in younger arteries to 1.10 in older subjects(Kamenskiy et al. 2016).

These results are in good agreement with experimental data reported previously. Smouse et.al. and Nikanorov et.al. (Smouse et al. 2005; Nikanorov et al. 2008) measured axial compression of 14% in the PA of 73±10 year old cadavers. Klein et.al. (Klein et al. 2009) reported 16% compression and their subjects were younger, i.e. 57±10 years old. MacTaggart et.al. (MacTaggart et al. 2014) measured 12±11% average compression with maximum values reaching 19% and 30% at the AH and in the PA of 76±19 year old cadavers. Finally, Poulson et.al. (Poulson et al. 2017) reported 25% maximum PA compression in 80±12 year old cadavers. Only one study measured axial compression in younger FPAs (20–36 year old) (Cheng et al. 2006) and found 13% compression; however these results were obtained for the more proximal SFA segment that compresses significantly less than the distal SFA–PA segments studied here(MacTaggart et al. 2014), which explains the lower values.

While calculated *in situ* compression discussed above correlates well with the experimentally measured values, it does not allow assessing the true stress-strain state experienced by the artery because of the presence of longitudinal pre-stretch. Pre-stretch is defined as the ratio of *in situ* artery length to its excised length, and therefore cannot be measured *in vivo*. Pre-stretch in the human FPA can be estimated based on subject's age(Kamenskiy et al. 2016), and it can be incorporated into a computational model to calculate the total (i.e. *excised*) axial deformation experienced by the artery during limb

flexion which includes both tension due to pre-stretch and compression due to limb flexion. Average excised axial deformation ranged from 15% tension for the youngest age group to 7% compression for the oldest age group with maximum values reaching 25% tension and 22% compression respectively. Arteries younger than 50 years of age experienced mostly tension during acute limb flexion, although direct imaging of *in situ* length would suggest compressive deformations. The same applies for computational models that do not take longitudinal pre-stretch into account. The fact that younger arteries are experiencing tension even in the acutely bent limb posture may explain their significantly straighter shapes in this posture than shapes of the older FPAs.

Our data demonstrate that longitudinal pre-stretch plays a paramount role in FPA mechanics, largely determining the shape that the artery assumes with limb flexion. Computational analysis suggests that young compliant arteries with low pre-stretch are more tortuous in the flexed limb posture than stiffer arteries of older subjects. While more research is needed to investigate these controversial findings, this result suggests that arterial stiffening can in fact act as a protective mechanism to strengthen the arterial wall and prevent it from kinking during limb flexion.

Tensile and compressive deformations may play important roles in FPA pathophysiology as mechanical stretch is known to regulate smooth muscle cell proliferation, apoptosis, phenotype, migration, alignment, and is known to stimulate extracellular matrix remodeling(Birukov 2009; Mantella et al. 2015). Frequency, amplitude, and pattern of mechanical stimulation can influence pro- or anti-inflammatory cell responses and may differentially regulate the remodeling processes. Though most attention has been given to studying the effects of high frequency cyclic mechanical stretch that is mostly pertinent to circumferential stretching imposed by the blood flow during the cardiac cycle, large deformations of the FPA during limb flexion and their effects on smooth muscle cell functions also deserve thorough investigation, particularly as the artery changes its deformations from tensile to compressive.

In addition to FPA deformations, aging also affects intramural stresses and changes their distribution along the length of the artery. Though FPA stress modeling is relatively unexplored, one previous study(Ní Ghriallais and Bruzzi 2013) has developed an anatomically accurate model of the limb that included bones, muscles, artery and skin. Authors have not considered pre-stretch, but have calculated Von Mises stresses and reported that they were higher distally in the PA below the knee which agrees with our findings. We further report that in younger arteries, maximum principal stress associated with limb flexion is distributed rather uniformly along the FPA length with higher values concentrated away from the bends. As the artery ages and loses pre-stretch, stresses redistribute and localize to the bends in the distal SFA around the AH, and in the PA below the knee–areas most commonly affected by the atherosclerotic disease(Watt 1965). Maximum principal stresses in these areas increase more than 3-fold with age with higher increases observed at the AH.

Similar trends with aging were also observed for the FPA hemodynamics demonstrating exponential increase in atheroprone TAWSS and OSI after 50 years of age, and a significant

reduction in atheroprotective TAWSS by 35 years of age. The effect of low and oscillatory shear has been extensively studied and is thought to include mediated recruitment of monocytes, increased vasoconstriction and paracrine growth stimulation of vessel wall constituents, increased oxidant state, and increased apoptosis and cellular turnover(Malek et al. 1999).

While present study can help better understand FPA pathophysiology and foster development of better devices and materials for PAD treatment, it must be considered in the context of its limitations. First, we have not considered effects of blood pressure in our solid model due to use of rigid rings for spring attachments. Although blood pressure would change stress values, it is unlikely that it will affect stress distribution or change the results related to the effect of age. Solid and fluid analyses were performed separately for the sake of simplicity and computational efficiency. While it is unlikely that fluid-structure interaction will change the results qualitatively, quantitative effects may still be sizable. Finally, all computational models need to be validated with experimental data. This will require a set of younger cadavers to assess the deformed shape that FPA takes with limb flexion and extension. Further work in this area is therefore warranted.

Acknowledgments

The authors wish to acknowledge the Charles and Mary Heider Fund for Excellence in Vascular Surgery for their help and support. Computational fluid dynamics simulations were carried out within the joint initiative of CINECA and the Lombardy region LISA under the project B-BeST (Bringing biomedical simulations to clinical target).

References

Adam DJ, Beard JD, Cleveland T, et al. Bypass versus angioplasty in severe ischaemia of the leg (BASIL): multicentre, randomised controlled trial. Lancet. 2005; 366:1925–34. DOI: 10.1016/S0140-6736(05)67704-5 [PubMed: 16325694]

Ansari F, Pack LK, Brooks SS, Morrison TM. Design considerations for studies of the biomechanical environment of the femoropopliteal arteries. J Vasc Surg. 2013; 58:804–813. DOI: 10.1016/j.jvs.2013.03.052 [PubMed: 23870198]

Antiga L, Piccinelli M, Botti L, et al. An image-based modeling framework for patient-specific computational hemodynamics. Med Biol Eng Comput. 2008; 46:1097–1112. DOI: 10.1007/s11517-008-0420-1 [PubMed: 19002516]

Birukov KG. Cyclic stretch, reactive oxygen species, and vascular remodeling. Antioxid Redox Signal. 2009; 11:1651–1667. DOI: 10.1089/ars.2008.2390 [PubMed: 19186986]

Cheng C, Wilson N, Hallett R. In vivo MR angiographic quantification of axial and twisting deformations of the superficial femoral artery resulting from maximum hip and knee flexion. J Vasc Interv Radiol. 2006; 17:979–987. DOI: 10.1097/01.RVI.0000220367.62137.E8 [PubMed: 16778231]

Cheng CP, Choi G, Herfkens RJ, Taylor Ca. The effect of aging on deformations of the superficial femoral artery resulting from hip and knee flexion: potential clinical implications. J Vasc Interv Radiol. 2010; 21:195–202. DOI: 10.1016/j.jvir.2009.08.027 [PubMed: 20022767]

Clowes AW, Reidy MA, Clowes MM. Mechanisms of stenosis after arterial injury. Lab Invest. 1983; 49:208–215. [PubMed: 6876748]

Conte MS, Bandyk DF, Clowes AW, et al. Results of PREVENT III: a multicenter, randomized trial of edifoligide for the prevention of vein graft failure in lower extremity bypass surgery. J Vasc Surg. 2006; 43:742–751. DOI: 10.1016/j.jvs.2005.12.058 [PubMed: 16616230]

Desyatova A, MacTaggart J, Poulson W, et al. The choice of a constitutive formulation for modeling limb flexion-induced deformations and stresses in the human femoropopliteal arteries of different

ages. Biomech Model Mechanobiol. 2017a; 16:775–785. DOI: 10.1007/s10237-016-0852-8 [PubMed: 27868162]

Desyatova, A., Poulson, W., Deegan, P., et al. Limb flexion-induced twist and associated intramural stresses In the human femoropopliteal artery. J R Soc Interface. 2017b. http://dx.doi.org/10.1098/rsif.2017.0025

Dunlop GR, Santos R. Adductor-Canal Thrombosis. N Engl J Med. 1957; 256:577–580. DOI: 10.1056/NEJM195703282561301 [PubMed: 13451898]

Greenwald S. Ageing of the conduit arteries. J Pathol. 2007; 211:157–172. DOI: 10.1002/path [PubMed: 17200940]

Higashiura W, Kubota Y, Sakaguchi S, et al. Prevalence, factors, and clinical impact of self-expanding stent fractures following iliac artery stenting. J Vasc Surg. 2009; 49:645–652. DOI: 10.1016/j.jvs.2008.10.019 [PubMed: 19268770]

Iida O, Nanto S, Uematsu M, et al. Effect of exercise on frequency of stent fracture in the superficial femoral artery. Am J Cardiol. 2006; 98:272–274. [PubMed: 16828607]

Jani B, Rajkumar C. Ageing and vascular ageing. Postgrad Med J. 2006; 82:357–62. DOI: 10.1136/pgmj.2005.036053 [PubMed: 16754702]

Kamenskiy A, Seas A, Bowen G, et al. In situ longitudinal pre-stretch in the human femoropopliteal artery. Acta Biomater. 2016; 32:231–237. DOI: 10.1016/j.actbio.2016.01.002 [PubMed: 26766633]

Kamenskiy A, Seas A, Deegan P, et al. Constitutive description of human femoropopliteal artery aging. Biomech Model Mechanobiol. 2017; 16:681–692. DOI: 10.1007/s10237-016-0845-7 [PubMed: 27771811]

Kamenskiy AV, Pipinos, Dzenis Ya, et al. Effects of age on the physiological and mechanical characteristics of human femoropopliteal arteries. Acta Biomater. 2015; 11:304–313. DOI: 10.1016/j.actbio.2014.09.050 [PubMed: 25301303]

Klein AJ, Chen SJ, Messenger JC, et al. Quantitative assessment of the conformational change in the femoropopliteal artery with leg movement. Catheter Cardiovasc Interv. 2009; 74:787–798. [PubMed: 19521998]

Lakatta EG, Wang M, Najjar SS. Arterial Aging and Subclinical Arterial Disease are Fundamentally Intertwined at Macroscopic and Molecular Levels. Med Clin North Am. 2009; 93:583–604. DOI: 10.1016/j.mcna.2009.02.008 [PubMed: 19427493]

Learoyd BM, Taylor MG. Alterations with Age in the Viscoelastic Properties of Human Arterial Walls. Circ Res. 1966; 18:278–292. DOI: 10.1161/01.RES.18.3.278 [PubMed: 5904318]

Lee H-Y, Oh B-H. Aging and Arterial Stiffness. Circ J. 2010; 74:2257–2262. DOI: 10.1253/circj.CJ-10-0910 [PubMed: 20962429]

MacTaggart J, Phillips N, Lomneth C, et al. Three-Dimensional Bending, Torsion and Axial Compression of the Femoropopliteal Artery During Limb Flexion. J Biomech. 2014; 47:2249–2256. [PubMed: 24856888]

Mahoney EM, Wang K, Cohen DJ, et al. One-year costs in patients with a history of or at risk for atherothrombosis in the United States. Circ Cardiovasc Qual Outcomes. 2008; 1:38–45. DOI: 10.1161/CIRCOUTCOMES.108.775247 [PubMed: 20031786]

Malek AM, Alper SL, Izumo S. Hemodynamics Shear Stress and Its Role in Atherosclerosis. JAMA. 1999; 282(21):2035–2042. [PubMed: 10591386]

Mantella LE, Quan A, Verma S. Variability in vascular smooth muscle cell stretch-induced responses in 2D culture. Vasc Cell. 2015; 7:7.doi: 10.1186/s13221-015-0032-0 [PubMed: 26301087]

Newcomer SC, Sauder CL, Kuipers NT, et al. Effects of posture on shear rates in human brachial and superficial femoral arteries. Am J Physiol Heart Circ Physiol. 2008; 294:H1833–9. DOI: 10.1152/ajpheart.01108.2007 [PubMed: 18245564]

Ní Ghriallais R, Bruzzi M. Effects of knee flexion on the femoropopliteal artery: A computational study. Med Eng Phys. 2013; 35:1620–8. DOI: 10.1016/j.medengphy.2013.05.015 [PubMed: 23810284]

Nikanorov A, Smouse HB, Osman K, et al. Fracture of self-expanding nitinol stents stressed in vitro under simulated intravascular conditions. J Vasc Surg. 2008; 48:435–440. DOI: 10.1016/j.jvs.2008.02.029 [PubMed: 18486426]

Nolan DR, Gower aL, Destrade M, et al. A robust anisotropic hyperelastic formulation for the modelling of soft tissue. J Mech Behav Biomed Mater. 2014; 39:48–60. DOI: 10.1016/j.jmbbm.2014.06.016 [PubMed: 25104546]

O'Rourke MF. Arterial aging: pathophysiological principles. Vasc Med. 2007; 12:329–41. DOI: 10.1177/1358863X07083392 [PubMed: 18048471]

Palma EC. Hemodynamic arteriopathy. Angiology. 1959; 10:134–43. [PubMed: 13661625]

Passerini T, Quaini A, Villa U, et al. Validation of an open source framework for the simulation of blood flow in rigid and deformable vessels. Int j numer method biomed eng. 2013; 29:1192–1213. DOI: 10.1002/cnm.2568 [PubMed: 23798339]

Patel DJ, Greenfield JC, Austen WG, et al. Pressure-flow relationships in the ascending aorta and femoral artery of man. J Appl Physiol. 1965; 20:459–463. [PubMed: 5319992]

Poulson W, Kamenskiy A, Seas A, et al. Limb Flexion-Induced Axial Compression and Bending in Human Femoropopliteal Artery Segments. J Vasc Surg. 2017; Accepted:1 7. doi: 10.1016/j.jvs.2017.01.071

Schillinger M, Sabeti S, Dick P, et al. Sustained benefit at 2 years of primary femoropopliteal stenting compared with balloon angioplasty with optional stenting. Circulation. 2007; 115:2745–9. DOI: 10.1161/CIRCULATIONAHA.107.688341 [PubMed: 17502568]

Schillinger M, Sabeti S, Loewe C. Balloon angioplasty versus implantation of nitinol stents in the superficial femoral artery. N Engl J Med. 2006; 354:1879–1888. [PubMed: 16672699]

Smouse BHB, Nikanorov A, Laflash D. Biomechanical Forces in the Femoropopliteal Arterial Segment. Endovasc Today. 2005:60–66.

Watt J. Origin of femoro-popliteal occlusions. Br Med J. 1965; 2:1455–1459. [PubMed: 5849435]

Wensing PJW, Meiss L, Mali WPTM, Hillen B. Early Atherosclerotic Lesions Spiraling Through the Femoral Artery. Arterioscler Thromb Vasc Biol. 1998; 18:1554–1558. DOI: 10.1161/01.ATV.18.10.1554 [PubMed: 9763526]

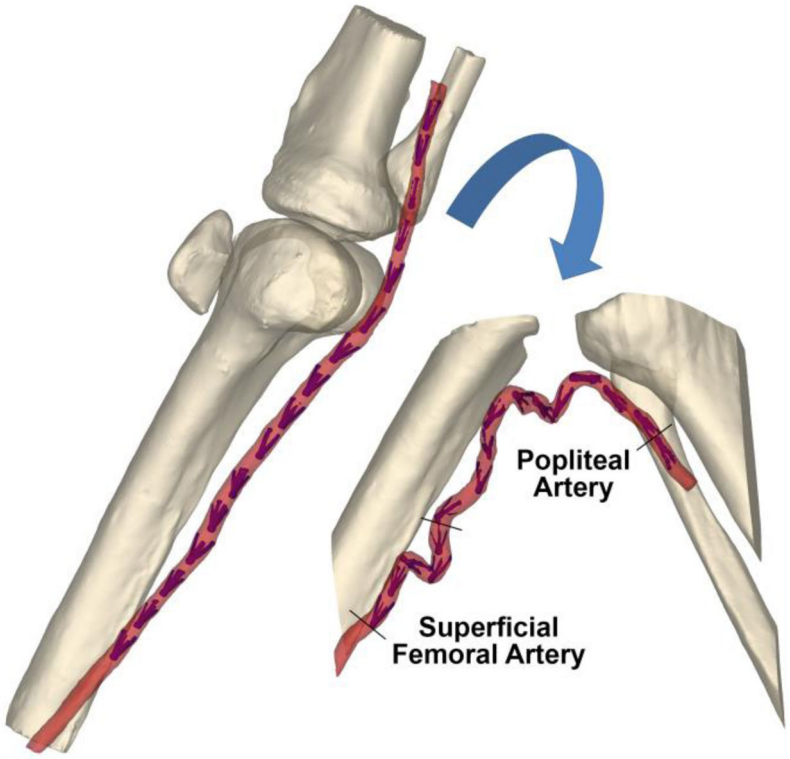

Figure 1.
3D reconstruction of the CT demonstrating limbs in the standing (180°, left) and gardening (60°, right) postures. Intra-arterial markers are colored blue.

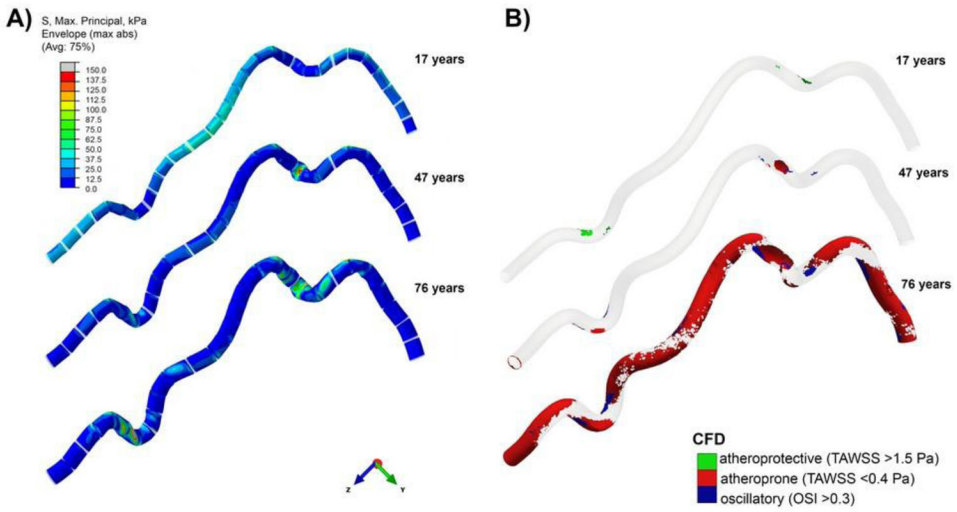

Figure 2.

Deformed shapes and A) distribution of maximum principal stresses (kPa) and B) blood flow in the FPAs of different ages during limb flexion. Results are presented for three age groups. Note that segments in panel A around rigid rings were not included in the stress analysis due to edge effects. Levels of atheroprotective and atheroprone TAWSS and OSI on panel B were defined according to Malek et el(Malek et al. 1999). Aging results in higher localization and increased magnitude of intramural stressess at the adductor hiatus and popliteal artery below the knee, as well as decrease in atheroprotective TAWSS, and increases in atheroprone TAWSS and OSI.

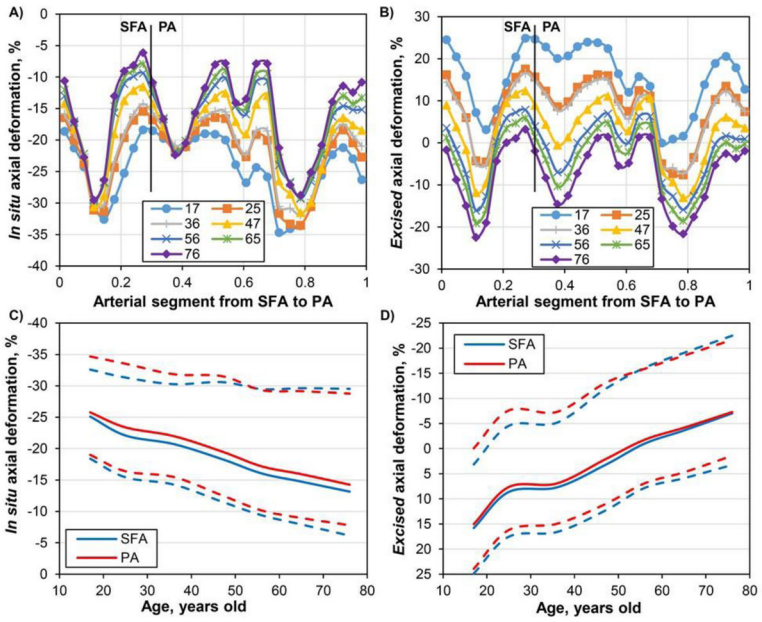

Figure 3.

Effects of age on the *in situ* (A, C) and *excised* (B, D) axial compressions of the FPA with limb flexion. Panels A and B demonstrate distribution of axial compression along the normalized length of the FPA for different age groups. Vertical line represents a formal division of the artery into the SFA and PA as demonstrated in Figure 1. AH is included in the distal SFA. Panels C and D demonstrate changes in axial deformations for the SFA and PA segments with age. Solid lines represent average values; dashed lines represent upper and lower limits for the segment. Positive values refer to tension, negative to compression.

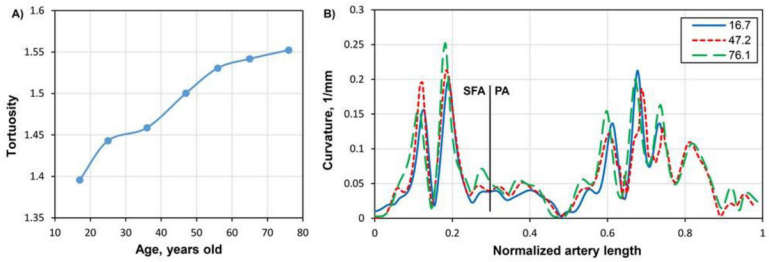

Figure 4.

A) Effect of age on the tortuosity of the FPA centerline in the flexed limb posture. B) Curvature of the FPA centerline for three age groups. Vertical line represents a division of the FPA into the SFA and PA as shown in Figure 1.

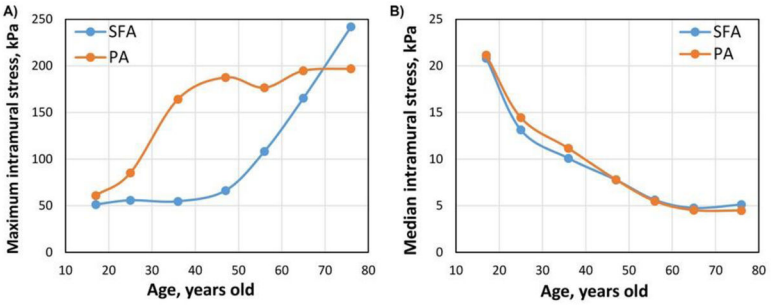

Figure 5.
Effect of age on maximum (A) and median (B) intramural stresses in the SFA and PA.

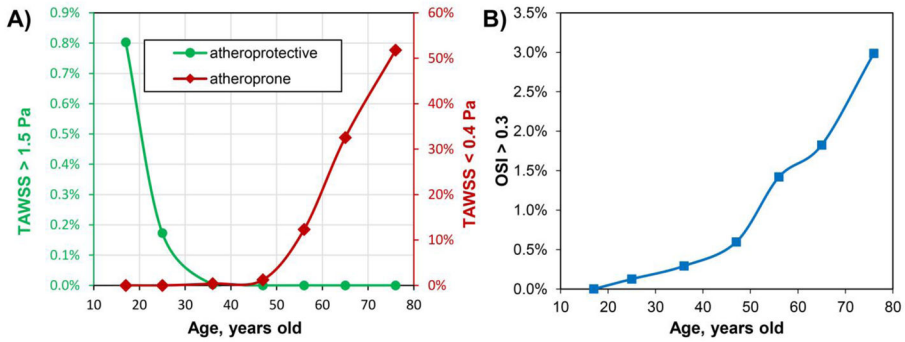

Figure 6.

Effect of age on TAWSS and OSI expressed as percent of the total FPA surface area. Note that atheroprotective TAWSS is significantly reduced by 35 years of age, atheroprone TAWSS starts to exponentially increase after 50 years of age, and OSI monotonically increases during the entire lifespan with an exponential rise after the age of 50 years.